Geometric determinants of the place fields of hippocampal neurons

John O'Keefe & Neil Burgess

Department of Anatomy, University College London, London WC1E 6BT, UK

The human hippocampus has been implicated in memory[1], in particular episodic[2,3] or declarative[4] memory. In rats, hippocampal lesions cause selective spatial deficits[2,5–7], and hippocampal complex spike cells (place cells) exhibit spatially localized firing[8,9], suggesting a role in spatial memory[2], although broader functions have also been suggested[10,11]. Here we report the identification of the environmental features controlling the location and shape of the receptive fields (place fields) of the place cells. This was done by recording from the same cell in four rectangular boxes that differed solely in the length of one or both sides. Most of our results are explained by a model in which the place field is formed by the summation of gaussian tuning curves, each oriented perpendicular to a box wall and peaked at a fixed distance from it.

Place cells were recorded from six rats foraging for food in four boxes (a small square, SS; large square, LS; horizontal rectangle, HR; and vertical rectangle, VR) located within a rectangular testing room oriented north–south (Fig. 1). We first investigated whether the location of peak firing in the different boxes reflected simple determinants, such as the distance to two orthogonal box walls, or the proportion of the distance between opposite walls. Three examples of place cells that fired in all four boxes are shown in Fig. 1. The location of the place fields shows a systematic relation across the boxes. Fields B and C occur at fixed distances from the closest two walls, while field D occurs at a fixed distance from the west wall and at a fixed ratio of the distance between the north and south walls.

We analysed 28 place fields from 27 well-isolated hippocampal complex spike (pyramidal) cells (one cell had two separate fields in all boxes). Most (81 of 112) of the firing rate maps (Fig. 1) showed one contiguous region of firing with a single peak; see

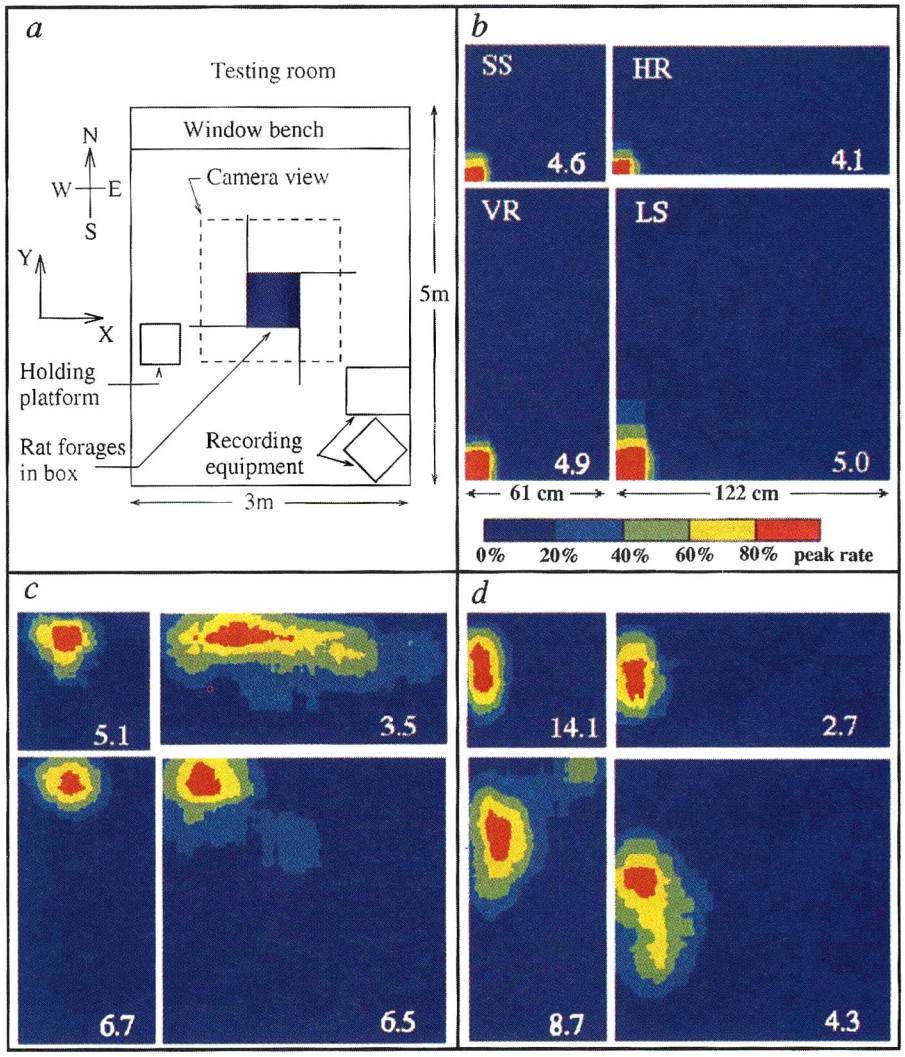

FIG. 1 *a*, Plan of the testing room and the location of the camera viewing region within it. Four boxes of different shapes were set within this space: a small square (shown in blue), a horizontal rectangle, a vertical rectangle and a large square. Each box was constructed from four identical grey planks (61 cm high, 122 cm long) fastened at the top by clamps. The planks and the paper floor covering were frequently changed to ensure that local olfactory and tactile cues made no consistent contribution to cell firing. Some trials were repeated with the box in a different room location to examine the effect of room features on the location of the place field. The SS measured 61 × 61 cm, the LS 122 × 122 cm and the two rectangles 61 × 122 cm. *b–d*, Location of place field. Firing rate maps for three place cells (*b* and *c*, from region CA1; *d*, from CA3). One 8-min trial in each of the boxes (indicated by the coloured region; SS, small square; HR, horizontal rectangle; VR, vertical rectangle; LS, large square) is shown. Across all 4-boxes, the location of the peak firing rate of the cell in *b* occurs at a fixed distance from the west wall (mean 3.5 cm, s.d. 0.5 cm) and south wall (2.7 ± 2.1 cm); the peak firing rate of the cell in *c* occurs at a fixed distance from the west wall (24.0 ± 6.4 cm) and from the north wall (11.7 ± 1.4 cm), and the peak firing rate of the cell in *d* occurs at a fixed distance from the west wall (9.4 ± 3.3 cm) and at a fixed ratio of the distance between north and south walls (0.64 ± 0.066). These measures are referred to as the determinants of the location of the place fields; see Table 1*b*.

METHODS. Recording techniques are as described[15]. Briefly, 6 rats were implanted with moveable 'tetrodes' (bundles of 4 microelectrodes) held in microdrives. Four rats were initially trained to forage in the VR, and two in the HR. During foraging the rat's location and unit activity from each tetrode were recorded. Spikes were identified by their waveform on the 4 electrodes. We selected well-isolated units, ensured that the same unit was recorded across trials by comparing waveforms, and identified recording sites as CA1 and CA3 fields of the hippocampus. Square bins 1/24 of the area of the current box were placed around grid points on the camera viewing area. The number of spikes fired by each cell and the time spent by the rat in each bin were recorded. The firing rate at each grid point is mapped as a colour plot with linear interpolation between grid points. The 5 colours, from dark blue to red, are autoscaled so that each represents 20% of the peak rate, shown in white in the corner of each plot. Fields with a peak rate of less than 1.0 Hz are not shown.

Table 1*a*. The locations of the peak firing rate in most of these place fields are determined by fixed distances or proportions of distances to a box wall in the directions defined by the axes of the box (38 of 56 determinants; see Table 1*b*). Beyond this, 3 of the 28 cells clearly had a determinant in one direction that was fixed to some aspect of the laboratory frame (the room walls are likely candidates, as the fields moved relative to the laboratory frame in the orthogonal direction without distortion; that is, the relevant room features must be extended and parallel to the box walls).

Place fields are not localized points but have two-dimensional structure. What determines their shape? For some cells, the shape of the field varied systematically between boxes differing in length along one direction: either stretching or revealing a second peak along that direction in the larger box (Table 1*a*). Figure 1*c* (SS and HR), *d* (HR and LS) shows fields stretching, and Fig. 2*a* (HR), *b* (LS) shows second peaks. Overall, 9 of 28 fields showed a second peak in one or more of the larger boxes. When examined, these secondary peaks accounted for some of the failures to find a determinant in the original analysis (Table 1*b*; Fig. 2*a*). The appearance of these place fields suggests a possible mechanism underlying their formation: small unitary fields might be composed of two or more independent subcomponents 'tied' at fixed distances to opposite walls; these fields then become pulled apart in one or more of the larger boxes. We examined the hypothesis that fields should be most compact in the box shape in which the animal was first trained, but found no clear evidence for this. Fields from rats initially trained in the VR, which stretch horizontally (Figs 1*c* and 2*a*), support this hypothesis, whereas fields from rats initially trained in the VR, which stretch vertically, do not (Figs 1*d* and 2*b*).

The firing rate of place cells does not usually depend on the rat's direction in open field environments, such as cylinders and squares[12,13], although it does in narrow-armed mazes[12,14] and linear tracks[15]. Many of the stretched and doubly peaked fields (22 of 24, from 14 of 15 cells) indicated a dramatic difference in the location of the peak firing rate according to the rat's direction of travel. In 13 of these (from 9 cells), the effect was straightforward: the peak of the field shifted towards the wall away from which the rat was moving. For example, if the field is stretched or split north–south (as in the LS in Fig. 2*b*), then when the rat is moving north the firing rate of the southern peak is much greater than when it is moving south, and vice versa for the northern peak. This effect is shown in Fig. 2*c*, *d* for the double fields in Fig. 2*a*, *b*. Our results suggest that the omnidirectional place fields seen in open field environments comprise several superimposed directional subcomponents.

We next considered the firing rates of the cells. Although these were consistent across boxes for many cells (Fig. 1*b*, *c*), they varied markedly for others (Fig. 2*a*, *b*). In some cases the peak rate fell below 1.0 Hz and no field was identified (Table 1*a*). Of 28 cells, 5 had fields in 2 of the 4 boxes, 9 had fields in 3, and 14 had fields in all 4. Of the 5 fields present in only 2 boxes, the boxes concerned varied in only one dimension, that is, fields never appeared solely in the SS and LS, nor solely in the HR and VR. This shows that the shape of the box *per se* was not a major determinant of the firing rate in the present experiment[16,17]. We hypothesized that the

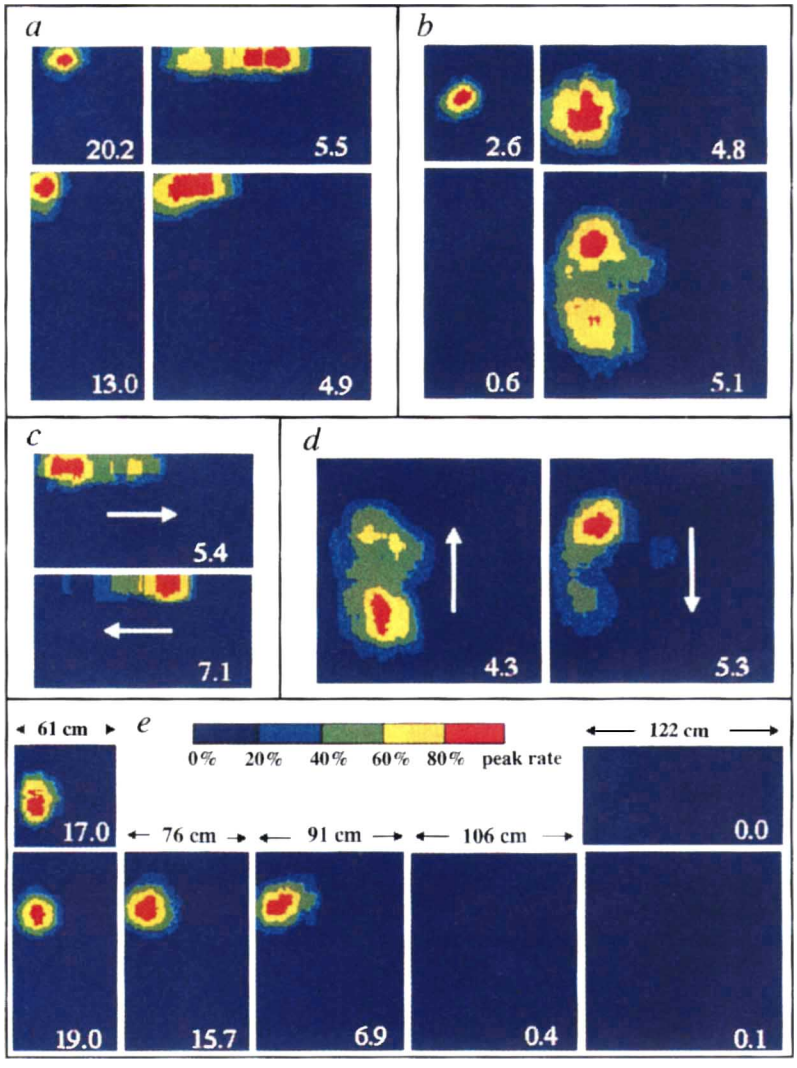

FIG. 2 Dissection of the place field. *a*, *b*, Examples of how separate subcomponents of a field tied to opposing walls can sometimes be observed being pulled apart as the box expands. *a*, CA1 place cell with fields exhibiting two separate subpeaks in the HR. The determinant of its location is the distance from the north wall (6.7 ± 1.8 cm) in the *Y* direction and is unknown in the *X* direction (although if the westmost subpeak in the HR is taken the *X* determinant becomes the distance from the west wall). *b*, CA3 place cell that fires in three of the four boxes with a field in the LS having two separate subpeaks. The distance form the west wall (24.9 ± 3.9 cm) is the *X* determinant of field location, and the distance from the north wall is the *Y* determinant (35.5 ± 6.2 cm). *c*, *d*, Firing rate maps of *a* (HR) and *b* (LS) when the rat's direction of travel is taken into account. These maps were constructed using only the positions and spikes acquired while the rat was moving in the direction shown by the white arrow ($\pm 90^\circ$). Two subcomponents of the field are revealed, with the stronger occurring earlier in the run in each case (when the rat runs away from the wall to which the location of the subcomponent is tied). Neither field was strongly modulated by the rat's direction of travel in the SS. These results imply that the small omnidirectional circular fields normally seen in open field environments may comprise superimposed directional subcomponents. e, This CA1 cell fired strongly in the SS and the VR, but not in the HR or LS. In further trials it was recorded in a series of boxes intermediate to the VR and LS: the cell's peak firing rate decreases monotonically with the *X* dimension of the box (while the *Y* dimension is held constant), until the rate is so low that the field disappears. Comparing locations of fields in the various boxes, including that in the SS, reveals that they remain at a fixed distance from the west wall of the box (15.1 ± 0.8 cm), and at a fixed distance from the north wall (36.5 ± 4.0 cm). These were accepted as determinants of the field location; see Table 1 legend.

absence of firing in some boxes might be the result of a gradual decrease in firing rate as a box dimension was increased or decreased owing to a reduction in the overlap of subcomponents associated with the opposing walls. There was evidence for this in the cell shown in Fig. 2*e*. This cell fired at a high rate in a restricted area of the SS and the VR, but did not fire in the LS or the HR. Recording in boxes intermediate to the VR and LS indicated that the peak firing rate was controlled by the width of the box. However, this simple hypothesis does not completely explain the firing rates observed in all trials (for example, in Fig. 2*b* the rate in the LS should be less than in the HR).

The shape and location of the place fields found in this study can be approximately modelled as a thresholded sum of the gaussian tuning-curve functions of the distance of the rat from each box wall, where tuning curves that peak far from a wall are broader and of lower amplitude than those that peak near to a wall (see Fig. 3 legend). In general, our model assumes four gaussian functions, but in principle any number would be possible. In some cases only two or three effective inputs make for a better fit (Fig. 3*a*, *d*), and some cells appear to receive inputs fixed to the testing room as well as those from box walls (see above). We found no cells with a single input (which would resemble a stripe or an edge field).

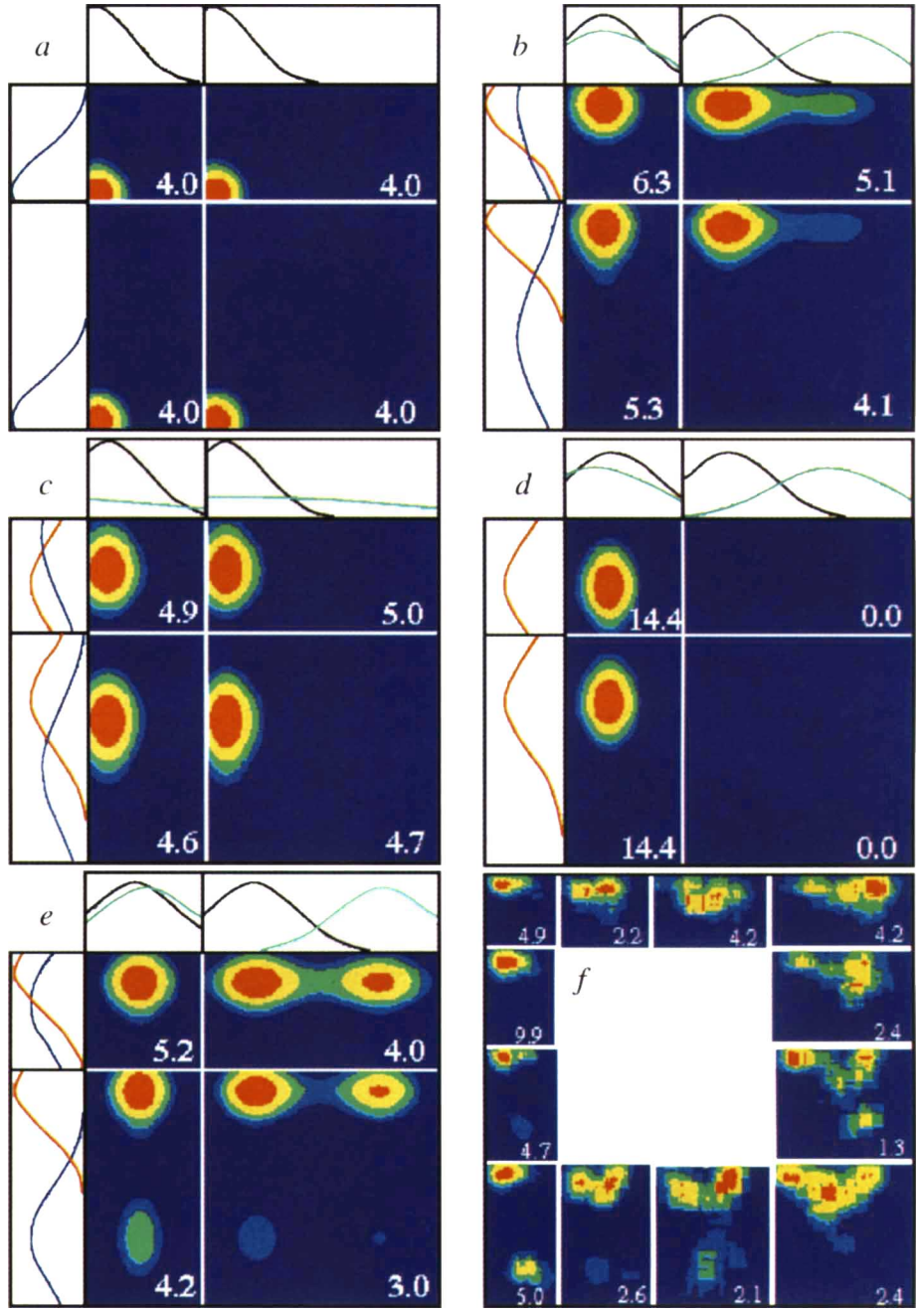

FIG. 3 A model of place fields. The main characteristics of place field shape and location can be modelled as a thresholded sum of gaussian tuning curves in the distance of the rat from each box wall. If the four corners of a box w cm by h cm are at $(0,0)$ $(w,0)$ $(0,h)$ and (w,h) then we can model a place cell's firing rate map $f(x, y)$, where (x, y) is the position of the rat and f is the cell's firing rate, as:

$$f(x,y) \approx A\left(\frac{\exp\{-[(h-y)-d_N]^2/2\sigma^2(d_N)\}}{\sqrt{[2\pi\sigma^2(d_N)]}} + \frac{\exp[-(y-d_S)^2/2\sigma^2(d_S)]}{\sqrt{[2\pi\sigma^2(d_S)]}} + \frac{\exp\{-[(w-x)-d_E]^2/2\sigma^2(d_E)\}}{\sqrt{[2\pi\sigma^2(d_E)]}} + \frac{\exp[-(x-d_W)^2/2\sigma^2(d_W)]}{\sqrt{[2\pi\sigma^2(d_W)]}}\right) - T,$$

where A gives the overall amplitude, T is a threshold, d_N is the value at which the tuning curve in the distance from the north wall peaks (in cm), d_S, d_W and d_E are defined similarly, and the width $\sigma(x)$ is an increasing function of x. Specifically, we have used $\sigma(x) = \sigma_0(61^2 + x^2)/61^2$ so that if the rat measures the distance x to a wall as, say, the angle from vertical to the top of the wall (61 cm high), then the width of the gaussian is constant under this measure of distance ($\sigma_0 = 20$ cm). Note that gaussians peaked close to a wall will be higher and narrower than those peaked far from one, owing to the variation in σ. The number of effective inputs may be made less than 4 by assigning large values to d_N, d_S, d_W or d_E. Colour plots show simulated firing rate maps, with the peak rate in white each corner, and the borders showing the gaussian tuning curves in the X and Y directions. *a*, Firing rate maps formed by summing two orthogonal gaussians in the 4 boxes. One curve is fixed to the west wall (black) and one to the south wall (blue). *b*, *c*, Summation of 4 gaussians, curves fixed to the east wall are shown in green and the north wall red. *a*–c, Simulations of the place fields in Fig. 1*b*–*d*, respectively, using a threshold T proportional to 80% of the peak firing rate in each box (showing the top 20% of the summed gaussian inputs in each box). *d*, Simulation of the cell in Fig. 2e, which fires in only 2 of the 4 boxes, using 3 inputs and a fixed threshold $T = 75$. Simulated fields appear in only 2 of the 4 boxes and would not appear solely in the SS and LS, or solely in the HR and VR, as in the data. *e*, *f*, Simulated and real data, respectively, in which a place field is pulled into more than 2 components as the box expands (the place cell in *f* was recorded in the 4 canonical boxes and 8 boxes of intermediate shape). The simulation in *e* used a threshold T proportional to 80% of the peak firing rate. In general, either of the above thresholding strategies (fixed across boxes, or proportional to the peak rate) may be necessary, or even a combination of them (as Fig. 2*b*). We suspect that absolute firing rates (and hence the choice of threshold) reflect variables other than the geometry of the environment, as well as local interactions with other place cells. Values of the parameters (A, d_N, d_S, d_E, d_W) were (500, 1,000, 5, 1,000, 5) for *a*, (500, 10, 50, 40, 20) for *b*, (500, 35, 50, 100, 10) for *c*, (2,000, 35, 1,000, 45, 25) for *d*, and (400, 10, 35, 30, 25) for *e*.

TABLE 1 Types of place field and the determinants of their location

(a) Number and type of place fields in each box

	Box shape				
Type of place field	SS	HR	VR	LS	Total
None	3	8	2	3	16
1 peak (stretched)	24 (1)	14 (2)	23 (4)	19 (4)	80 (11)
2 peaks	0	5	3	5	13
> 2 peaks	1	1	0	1	3
Total	28	28	28	28	112

(b) Frequency of the determinants of location

Dimension		x				
	Determinant	West wall	East wall	Proportion west–east	Unknown	Total
y	South wall	1	1	2	1	5
	North wall	4	0	4	3	11
	Proportion south–north	1	1	0	1	3
	Unknown	2	2	1	4	9
	Total	8	4	7	9	28

In *a*, 'None' indicates that the firing rate never exceeds 1.0 Hz; 'stretched' indicates singly peaked fields judged by eye to be at least as stretched as that in the LS in Fig. 1*d*; '2 peaks' indicates fields with two regions of elevated firing separated by at least half of the total width of the field (the field in the HR in Fig. 2*a* is an example of the minimum separation); '> 2 peaks' indicates more than two regions of elevated firing all with this separation. In *b*, the 'field location' in each box was the location of the peak in the firing rate map; see Fig. 1. Firing-rate maps containing no field or more than 2 peaks (see Table 1*a*) were excluded; the higher peak was used in those with 2 peaks. The determinant of the field location in a particular direction was defined as a measure with a standard deviation across boxes σ small enough to be achieved in less than 5% of Monte Carlo simulations of the measure applied to randomly placed fields, that is, σ is within a 95% confidence interval, equivalently $P < 0.05$. We examined three measures in each direction: the distance to each of the two walls perpendicular to that direction, and the proportion of the distance from one wall to the other. If more than one measure qualified as a determinant (17 of 56 cases, all a distance and a proportion for a field near to a box wall), the one corresponding to the highest confidence was taken. Determinants were scored as 'unknown' either because none of the measures were determinants (15 of 18), or because there were no fields in boxes that varied in size along the relevant direction (3 of 18). The 95% confidence interval for distances varied from $\sigma < 2.3$ cm for a field present in two boxes to $\sigma < 11.1$ cm for a field in all four boxes, that for proportions varied from $\sigma < 0.018$ to $\sigma < 0.113$. Further simulations showed that $P < 0.15$ for finding one or more determinants among the three measures in a direction, and $P < 0.00001$ for finding 38 determinants of a possible 56. Where more than one trial was performed in a particular box, the firing-rate map with the highest peak rate was used for analysis and illustrations. Of the nine fields showing two peaks in one or more boxes, six originally lacked a determinant in one or more dimensions. In 4 of these, the second peak provided the missing determinant; for example, the distance from the west wall is a determinant of the field in Fig. 2*a* when the westmost subpeak in the HR is considered.

As the separation of two opposite walls is varied, this model predicts fields that peak at a fixed distance from a wall, fields that appear to peak at a fixed proportion of the distance between two walls, or fields that become stretched or pulled apart (using a threshold proportional to the peak rate; see Fig. 3*a*–*c*). If an absolute threshold is used across all trials, it can explain fields that disappear above or below critical values of the separation of opposing walls (Fig. 3*d*). In the extreme case the model predicts that a unitary field in the SS may be pulled into three or four components as the box expands, each a fixed distance from two of the walls (Fig. 3*e*). Data consistent with this were observed in the cell in Fig. 3*f*.

Place cells appear to identify environmental features such as the walls of the box on the basis of their sensory qualities and allocentric directions from the rat. Interchanging the planks that form the walls of a box, or rotating the box floor, did not alter the place field, ruling out a primary role for local odours or textures. The allocentric directions may derive from 'head-direction' cells[18], which might be determined by room features or by inertial (possibly vestibular) signals[19,20].

Our model builds on previous theoretical work[19,21–25], but emphasizes the importance of extended cues in given allocentric directions and, in particular, the walls bounding the environment (see refs 16,17). Experimental work consistent with our model includes the demonstration that place fields can expand when box size is increased[26], and that fields can be shifted by changing the location of the start box on a linear track[27] (or in a two-dimensional environment if the field is in or near the start box[28]). The directionality observed in the stretched and doubly peaked fields is consistent with an exaggerated form of the observation that place fields are more compact when each spike is considered to code for a future position of the rat[29]. Our results may help to explain those of previous experiments in which gerbils searched in two separate locations after two cues indicating a single reward site were pulled apart[30]. Finally, we have started to develop a quantitative understanding of how environmental features drive the firing of place cells. This should allow a more quantitative basis to be used for spatial theories of hippocampal function, and may have implications for cognitive map theory[2]. □

Received 8 November 1995; accepted 19 March 1996.

1. Scoville, W. B. & Milner, B. *J. Neurol. Neurosurg. Psychiat.* **20,** 11–21 (1957).
2. O'Keefe, J. & Nadel, L. *The Hippocampus as a Cognitive Map* (Clarendon, Oxford, 1978).
3. Tulving, E. *Elements of Episodic Memory* (Clarendon, Oxford, 1983).
4. Squire, L. R. *J. cogn. Neurosci.* **4,** 232–243 (1992).
5. O'Keefe, J., Nadel, L., Keightley, S. & Kill, D. *Expl Neurol.* **48,** 152–166 (1975).
6. Morris, R. G. M., Garrard, P., Rawlins, J. N. P. & O'Keefe, J. *Nature* **297,** 681–683 (1982).
7. Sutherland, R. J., Kolb, B. & Whishaw, I. *Neurosci. Lett.* **31,** 271–276 (1982).
8. O'Keefe, J. & Dostrovsky, J. *Brain Res.* **34,** 171–175 (1971).
9. O'Keefe, J. *Expl Neurol.* **51,** 78–109 (1976).
10. Eichenbaum, H. *J. cogn Neurosci.* **4,** 217–231 (1992).
11. Rudy, J. W. & Sutherland, R. J. *Hippocampus* **5,** 375–389 (1995).
12. Muller, R. U., Bostock, E., Taube, J. S. & Kubie, J. L. *J. Neurosci.* **14,** 7235–7251 (1994).
13. O'Keefe, J. *Prog. Neurobiol.* **13,** 419–439 (1979).
14. McNaughton, B. L., Barnes, C. A. & O'Keefe, J. *Expl Brain Res.* **52,** 41–49 (1983).
15. O'Keefe, J. & Recce, M. *Hippocampus* **3,** 317–330 (1993).
16. Cheng, K. *Cognition* **23,** 149–178 (1986).
17. Margules, J. & Gallistel, C. R. *Anim. Learn. Behav.* **16,** 404–410 (1988).
18. Taube, J. S., Muller, R. U. & Ranck, J. B. *J. Neurosci.* **10,** 420–435 (1990).
19. McNaughton, B. L., Knierim, J. J. & Wilson, M. A. in *The Cognitive Neurosciences* (ed. Gazzaniga, M.) 585–596 (MIT Press, Boston, 1994).
20. Knierim, J. J., Kudrimoti, H. S. & McNaughton, B. L. *J. Neurosci.* **15,** 1648–1659 (1995).
21. Zipser, D. *Behavl. Neurosci.* **99,** 1006–1018 (1985).
22. Sharp, P. E. *Psychobiology* **19,** 103–115 (1991).
23. O'Keefe, J. in *Brain and Space* (ed. Paillard, J.) 273–295 (Oxford Univ. Press, 1991).
24. Burgess, N., Recce, M. & O'Keefe, J. *Neural Networks* **7,** 1065–1081 (1994).
25. Redish, A. D. & Touretzky, D. S. in *Symbolic Visual Learning* (eds Ikeuchi, K. & Veloso, M.) (Oxford Univ. Press) (in the press).
26. Muller, R. U. & Kubie, J. L. *J. Neurosci.* **7,** 1951–1968 (1987).
27. Gothard, K. M., Skaggs, W. E. & McNaughton, B. L. *Soc. Neurosci. Abstr.* **21,** 911 (1995).
28. Gothard, K. M., Skaggs, W. E., Moore, K. M. & McNaughton, B. L. *J. Neurosci.* **16,** 823–835 (1996).
29. Muller, R. U. & Kubie, J. L. *J. Neurosci.* **9,** 4101–4110 (1989).
30. Collett, T. S., Cartwright, B. A. & Smith, B. A. *J. comp. Physiol. A* **158,** 835–851 (1986).

ACKNOWLEDGEMENTS. A preliminary version of this paper was presented at the Annual Meeting of the Society for Neuroscience (abstract 376.6, 1995). We thank E. Zohary for help in collecting some of the early data, K. Jeffery and J. Donnett for reading this manuscript, and C. Parker for technical assistance. This research was supported by the U.K. Medical Research Council. N.B. is a Royal Society university research fellow.

CORRESPONDENCE and requests for materials should be addressed to J.O'K. (e-mail: j.okeefe@.ucl.ac.uk).